Free Radical Biology and Medicine 71 (2014) 270–280

Contents lists available at ScienceDirect

Free Radical Biology and Medicine

journal homepage: www.elsevier.com/locate/freeradbiomed

Original Contribution

Redox proteomics analysis of HNE-modified proteins in Down syndrome brain: clues for understanding the development of Alzheimer disease

Fabio Di Domenico [a], Gilda Pupo [a], Antonella Tramutola [a], Alessandra Giorgi [a], Maria Eugenia Schininà [a], Raffaella Coccia [a], Elizabeth Head [b], D. Allan Butterfield [b,c], Marzia Perluigi [a,*]

[a] Department of Biochemical Sciences, Sapienza University of Rome, 00185 Rome, Italy
[b] Sanders-Brown Center on Aging, University of Kentucky, Lexington, KY 40506-0055, USA
[c] Department of Chemistry and Center of Membrane Sciences, University of Kentucky, Lexington, KY 40506-0055, USA

ARTICLE INFO

Article history:
Received 20 January 2014
Received in revised form
4 March 2014
Accepted 18 March 2014
Available online 25 March 2014

Keywords:
Protein oxidation
Down syndrome
Alzheimer disease
Redox proteomics
Lipid peroxidation
HNE
Trisomy 21
Free radicals

ABSTRACT

Down syndrome (DS) is the most common genetic cause of intellectual disability, due to partial or complete triplication of chromosome 21. DS subjects are characterized by a number of abnormalities including premature aging and development of Alzheimer disease (AD) neuropathology after approximately 40 years of age. Several studies show that oxidative stress plays a crucial role in the development of neurodegeneration in the DS population. Increased lipid peroxidation is one of the main events causing redox imbalance within cells through the formation of toxic aldehydes that easily react with DNA, lipids, and proteins. In this study we used a redox proteomics approach to identify specific targets of 4-hydroxynonenal modifications in the frontal cortex from DS cases with and without AD pathology. We suggest that a group of identified proteins followed a specific pattern of oxidation in DS vs young controls, probably indicating characteristic features of the DS phenotype; a second group of identified proteins showed increased oxidation in DS/AD vs DS, thus possibly playing a role in the development of AD. The third group of comparison, DS/AD vs old controls, identified proteins that may be considered specific markers of AD pathology. All the identified proteins are involved in important biological functions including intracellular quality control systems, cytoskeleton network, energy metabolism, and antioxidant response. Our results demonstrate that oxidative damage is an early event in DS, as well as dysfunctions of protein-degradation systems and cellular protective pathways, suggesting that DS subjects are more vulnerable to oxidative damage accumulation that might contribute to AD development. Further, considering that the majority of proteins have been already demonstrated to be oxidized in AD brain, our results strongly support similarities with AD in DS.

Down syndrome (DS) is one of the most frequent chromosomal abnormalities, resulting from the triplication of the part of chromosome 21 [1–5] that causes intellectual disability. In addition to cognitive deficits, individuals with DS show signs of premature aging, immune disorders, and other clinical pathologies [6]. By 35–40 years of age, a marked accumulation of senile plaques (SPs) and neurofibrillary tangles, the common neuropathological features of Alzheimer disease (AD), can be observed in DS brain [7,8]. Interestingly, there are reports of diffuse SPs in 8- to 12-year-old persons with DS [9,10], in whom the onset of dementia appears later, after 50 years of age, suggesting a prodromal period in which clinical signs are undetectable or minimal [11]. By studying autopsy samples from individuals with DS of various ages provides critical information regarding AD pathogenesis. Several studies showed that oxidative stress (OS) plays an important role in DS pathogenesis and in the development of AD pathology [12–15]. A recent study from our group reported increased OS conditions in brain of young DS people as indexed by increased carbonylation of specific proteins in the frontal cortex of DS subjects compared with non-DS cases [15]. Oxidative damage targets primarily proteasome and autophagy systems and may contribute to the disturbance of the proteostasis network in DS, thus potentially contributing to the development of AD [16]. Increased OS in DS most likely occurs as a consequence of overexpression of a subset of genes encoded by chromosome 21; among these, the most relevant

* Corresponding author. Fax: +39 064440062.
E-mail address: Marzia.perluigi@uniroma1.it (M. Perluigi).

http://dx.doi.org/10.1016/j.freeradbiomed.2014.03.027
0891-5849/

as potent OS inducers are APP (amyloid precursor protein) and SOD1 (superoxide dismutase 1). APP is the protein from which Aβ(1–42) peptide, the major protein in SPs in both DS and AD, is produced and Aβ(1–42) has been demonstrated to cause OS [17,18]. SOD1 has an important role in antioxidant defense, catalyzing the dismutation of $O_2^{\bullet -}$ to molecular oxygen and H_2O_2, the latter being decomposed in water by glutathione peroxide (GPX) and catalase (CAT). In DS the triplication of chromosome 21 leads to an increased production of H_2O_2, which is not followed by a similar increase in CAT and GPX, thus leading to an accumulation of H_2O_2 [19–21]. This compound, through the reaction with the reduced form of redox-active transition metal ions, leads to the formation of the hydroxyl radicals that are able to react and damage biological macromolecules, such as DNA, lipids, and proteins. In addition, superoxide can also react with nitric oxide, leading to the formation of peroxynitrite and other reactive nitrogen species.

In conditions of oxidative/nitrosative stress, proteins are highly vulnerable and may be the target of a number of modifications that may affect their functions. Further, if the oxidized proteins are not properly repaired or removed, they may accumulate within cells and become toxic. Different types of oxidative modifications, including, among others, carbonylation, formation of mixed disulfides, nitration, and formation of adducts with lipid peroxidation products, can be detected as indexes of tissue-specific damage.

Lipid peroxidation is one of the main events causing redox imbalance and subsequent buildup of oxidative stress within the cell. Lipid peroxidation is able to directly damage membranes, but reactive oxygen species (ROS) can also interact with polyunsaturated fatty acids, leading to the formation of copious amounts of reactive electrophilic aldehydes that are able to covalently bind proteins by forming adducts with specific amino acids [22]. According to a series of factors, such as acyl chain length and degree of unsaturation, the lipid hydroperoxide that is formed by reaction of a carbon radical with oxygen can decompose to produce reactive products such as malondialdehyde, 4-hydroxy-2-*trans*-nonenal (HNE), and acrolein. HNE is one of the most abundant and toxic aldehydes generated through ROS-mediated peroxidation of lipids and it is a highly reactive electrophile [23]. HNE can accumulate in cells and cause cell toxicity, membrane damage, disruption of Ca^{2+} homeostasis, and cell death and, with the other toxic aldehydes, is elevated in several neurodegenerative disease [24]. This compound can covalently modify protein residues of cysteine, lysine, and histidine by Michael addition, altering protein structure and causing loss of function and activity [25,26].

In this study, we investigated the role of lipid peroxidation in DS to shed light on the molecular mechanisms that may trigger the development of AD in DS subjects. Redox proteomics approaches [15] were used to analyze the frontal cortex of DS brain with and without AD pathology compared with age-matched controls to identify HNE-modified brain proteins.

Materials and methods

Subjects

DS, DS with AD pathology (DS/AD), and age-matched young (CTRY) and old (CTRO) control cases (six for each group) were obtained from the University of California at Irvine Alzheimer's Disease Research Center Brain Tissue Repository. Table 1 shows the characteristics and demographic data of all included subjects in the study. All DS cases were under the age of 40, whereas all cases with both DS and AD were over the age of 40. Thus, for this study, controls were split into two groups, either less than or equal to 40 years or older than 40 years of age at death. The postmortem interval (PMI) was different across groups, 9.96 ± 2.88 h for young controls, 12.5 ± 1.51 h for DS, 5.4 ± 2.8 h for DS/AD, and 8.9 ± 6.2 h for old controls. Subgroups used in this study were selected to maintain homogeneous age and gender inside the groups and were part of the entire cohort used in a previous experiment to investigate insoluble Aβ and total oxidation as a function of age in DS [15].

Sample preparation

Brain tissues (frontal cortex, around 20 mg per sample) from DS, DS/AD, and controls (six per group) were homogenized in Media 1 lysis buffer (pH 7.4) containing 320 mM sucrose; 1% of 990 mM Tris–HCl (pH 8.8); 0.098 mM $MgCl_2$; 0.076 mM EDTA; the proteinase inhibitors leupeptin (0.5 mg/ml), pepstatin (0.7 μg/ml), aprotinin (0.5 mg/ml), and phenylmethanesulfonyl fluoride (40 μg/ml); and phosphatase inhibitor cocktail (Sigma–Aldrich, St. Louis, MO, USA). Homogenates were centrifuged at 14,000 *g* for 10 min to remove debris. Protein concentration in the supernatant was determined by the Bradford assay (Pierce, Rockford, IL, USA).

Measurement of total protein-bound HNE

For the analysis of HNE-bound protein levels, 10 μl of frontal cortex homogenate was incubated with 10 μl of Laemmli buffer containing 0.125 M Tris base, pH 6.8, 4% (v/v) sodium dodecyl sulfate (SDS), and 20% (v/v) glycerol. The resulting samples (250 ng per well) were loaded onto a nitrocellulose membrane with a slot-blot apparatus under vacuum pressure. The membrane was blocked for 2 h with a solution of 3% (w/v) bovine serum albumin in phosphate-buffered saline containing 0.01% (w/v) sodium azide and 0.2% (v/v) Tween 20 and incubated with a rabbit polyclonal anti-4-hydroxynonenal antibody (1:3000; HNE-13M, Alpha Diagnostics, San Antonio, TX, USA) for 2 h at room temperature. This antibody specifically recognizes HNE-modified proteins. Membranes were washed and incubated with anti-rabbit IgG alkaline phosphatase secondary antibody (1:5000; Sigma–Aldrich) for 1 h at room temperature. Blots were dried and scanned by GS-800 densitometer (Bio-Rad) and analyzed by Quantity One (4.6.9 version; Bio-Rad, Hercules, CA, USA).

Two-dimensional (2D) electrophoresis

Brain sample proteins (200 μg) were precipitated in a 15% final concentration of trichloroacetic acid for 10 min in ice. Subsequently each sample was centrifuged at 10,000 *g* for 5 min and precipitates were washed in ice-cold ethanol:ethyl acetate 1:1 solution three times. The final pellet was dissolved in 200 μl rehydration buffer (8 M urea, 20 mM dithiothreitol (DTT), 2.0% (w/v) Chaps, 0.2% Bio-Lyte, 2 M thiourea, and bromophenol blue). First-dimension electrophoresis (isoelectric focusing) was performed with ReadyStrip IPG strips (11 cm, pH 3–10; Bio-Rad) at 300 V for 2 h linearly, 500 V for 2 h linearly, 1000 V for 2 h linearly, 8000 V for 8 h linearly, and 8000 V for 10 h rapidly. All the above processes were carried out at room temperature. After the first-dimension run the strips were equilibrated two times, first for 10 min in 50 mM Tris–HCl (pH 6.8) containing 6 M urea, 1% (w/v) SDS, 30% (v/v) glycerol, and 0.5% DTT and again for another 10 min in the same buffer containing 4.5% iodoacetamide in place of DTT. The second dimension was performed using 12% precast Criterion gels (Bio-Rad). The gels were incubated in fixing solution (7% acetic acid, 10% methanol) for 45 min and then stained for 1 h in Bio-Safe Coomassie gel stain (Bio-Rad) and destained overnight in deionized water. The Coomassie gels were scanned using a GS 800 densitometer (Bio-Rad).

Table 1
Individual demographic data.

Subject	PMI	Age	Sex	Race	Cause of death
Control Y 1	5.8	39	Female	Unknown	Unknown
Control Y 2	12	22.8	Male	African American	Arrhythmia due to hypertrophy cardiomyopathy
Control Y 3	8	33.1	Male	Caucasian	Cardiac arrhythmia
Control Y 4	10	24.4	Male	Caucasian	Multiple injuries
Control Y 5	10	10.8	Female	Caucasian	Asthma
Control Y 6	14	19.8	Male	Caucasian	Multiple injuries
Control Y	9.96 ± 2.88	24.9 ± 9.95	4 M, 2 F	1 AA, 4 Ca	
DS 1	12	1.9	Male	Caucasian	Unknown
DS 2	14	15.5	Male	Caucasian	Chromosome disorder, trisomy 21
DS 3	10	40.6	Male	African American	Hypertensive cardiovascular disease
DS 4	12	39.2	Female	Caucasian	Cancer
DS 5	13	44.5	Female	Caucasian	Cardiac arrhythmia
DS 6	14	19.9	Male	Indian	Cardiopulmonary arrest, congenital heart disease
DS	12.5 ± 1.51	26.9 ± 17.04	4 M, 2 F	1 AA, 4 Ca, 1 In	
DS/AD 1	5.3	57	Female	Unknown	Seizure disorder
DS/AD 2	3	63	Female	Unknown	Respiratory
DS/AD 3	6	63	Female	Unknown	Unknown
DS/AD 4	4.5	55	Male	Unknown	Pneumonia
DS/AD 5	10.5	61	Male	Unknown	Unknown
DS/AD 6	3	57	Female	Unknown	Pneumonia
DS/AD	5.4 ± 2.8	59.3 ± 3.44	2 M, 4 F		
Control O 1	5	47.3	Female	Caucasian	Pneumonia
Control O 2	8	64	Female	Unknown	Myocardial infarction
Control O 3	17	56.8	Male	Caucasian	Hypertensive arteriosclerotic cardiovascular disease
Control O 4	16	55.3	Male	Caucasian	Arteriosclerotic cardiovascular disease
Control O 5	4.5	65	Male	Unknown	Cardiac arrest
Control O 6	2.7	67	Male	Unknown	Cardiomyopathy
Control O	8.9 ± 6.2	59.2 ± 7.48	4 M, 2 F	3 Ca	

PMI, postmortem interval. AA, African American; Ca, Caucasian; In, Indian.

2D Western blot

For 2D Western blot, 2D gels (200 μg of proteins) were blotted onto nitrocellulose membranes (Bio-Rad) and HNE–protein adducts were detected on the membranes. Briefly, membranes were blocked for 1 h with 3% albumin in Tris-Buffered Saline and Tween 20 (T-TBS) and incubated with the primary mouse monoclonal anti-HNE antibody (1:500; Alpha Diagnostics) for 2 h at room temperature. After being washed with T-TBS three times for 5 min, the membranes were further incubated at room temperature for 1 h with the secondary antibody alkaline phosphatase-conjugated anti-mouse IgG (1:5000; Sigma–Aldrich). Membranes were then washed with T-TBS three times and developed using 5-bromo-4-chloro-3-indolyl phosphate/nitroblue tetrazolium solution.

Image analysis

2D gels and 2D blots (24 gels and 24 blots) were analyzed by PD-Quest 2D Analysis (7.2.0 version; Bio-Rad). PD-Quest spot-detection software allows the comparison of 2D gels as well as 2D blots from different groups. Powerful automatching algorithms quickly and accurately match gels or blots and sophisticated statistical analysis tools identify experimentally significant spots. The intensity value for each spot from an individual gel is normalized using the average mode of background subtraction. This intensity is afterward compared between groups using statistical analysis. Statistical significance was assessed using a two-tailed Student t test. p values < 0.05 were considered significant for comparison between control and experimental data (CTR vs DS). PD-Quest software allows normalization of a carbonylated spot's intensity on the blot for expression level of the same spot on the gel.

Trypsin digestion and protein identification by mass spectrometry

Protein spots identified to be statistically different from controls after PD-Quest analysis were digested in-gel by trypsin. Briefly, spots of interest were excised and then washed with 0.1 M ammonium bicarbonate (NH_4HCO_3) at room temperature for 15 min. Acetonitrile was added and incubated at room temperature for 15 min. This solvent mixture was then removed and the gel pieces were dried. The protein spots were then incubated with 20 ml of 20 mM DTT in 0.1 M NH_4HCO_3 at 56 °C for 45 min. The DTT solution was removed and replaced with 20 ml of 55 mM iodoacetamide in 0.1 M NH_4HCO_3. The solution was then incubated at room temperature for 30 min. The iodoacetamide was removed and replaced with 0.2 ml of 50 mM NH_4HCO_3 at room temperature for 15 min. Acetonitrile (200 ml) was added. After 15 min incubation, the solvent was removed, and the gel spots were dried for 30 min. The gel pieces were rehydrated with 20 ng/ml modified trypsin (Promega, Madison, WI, USA) in 50 mM NH_4HCO_3 with the minimal volume necessary to cover the gel pieces. The gel pieces were incubated overnight at 37 °C in a shaking incubator. Protein spots of interest were excised and subjected to in-gel trypsin digestion, and the resulting tryptic peptides were analyzed with MALDI-ToF. MALDI-ToF MS analyses were performed with an AutoFlex II instrument (Bruker Daltonics, Bremen, Germany), equipped with a 337 nm nitrogen laser and operating in reflector positive mode. Two tryptic autolytic peptides were used for the internal calibration (m/z 842.5100 and 2807.3145). Data were analyzed by flex Analysis program (Bruker Daltonics, Bremen, Germany). Identification by peptide mass fingerprint (PMF), with the mono-isotopic mass list, was performed using Bio Tools program (Bruker Daltonics, Bremen, Germany), by the Mascot search engine, against human SwissProt database [(SwissProt 2014_02 (542503 sequences)]. Up to two missed cleavage, 50 ppm measurement tolerance, oxidation at

methionine (variable modification) and carbamidomethylation at cysteine (fixed modification) were considered. Identifications were validated when the probability-based Mowse protein score was significant according to Mascot.

Western blot

For Western blot, 40 μg of proteins (CTRY, CTRO, and DS with and without AD) was separated by 12% SDS–PAGE and blotted onto a nitrocellulose membrane (Bio-Rad). The membrane was blocked with 3% bovine serum albumin in T-TBS and incubated for 1 h and 30 min at room temperature with primary anti-SOD1 (1:500; Santa Cruz Biotechnology, Dallas, TX, USA) and for 1 h at room temperature with secondary antibody horseradish peroxidase-conjugated anti-mouse IgG (1:5000; Sigma–Aldrich). The membrane was developed with the SuperSignal West Pico chemiluminescence substrate (Thermo Scientific, Waltham, MA, USA), acquired with Chemi-Doc MP (Bio-Rad), and analyzed using Image Lab software (Bio-Rad).

Immunoprecipitation of 78-kDa glucose-regulated protein (GRP78)

To confirm the correct identification of the proteins determined by MS, the identification of GRP78 was validated using immunochemical methods. Samples (100 μg of proteins) were incubated overnight with immunoprecipitation buffer (500 μl) and the antibody anti-GRP78, followed by 2 h of incubation with protein G–Sepharose beads, and then washed three times with RIA buffer. Proteins were separated by SDS–PAGE followed by immunoblotting on a nitrocellulose membrane (Bio-Rad). Membranes were incubated with the antibody anti-HNE and then detected by the peroxidase-conjugated secondary antibody (1:5000; Sigma–Aldrich) with SuperSignal West Pico chemiluminescence substrate (Thermo Scientific). Membranes were then acquired with Chemi-Doc MP (Bio-Rad) and analyzed using Image Lab software (Bio-Rad).

Native gel electrophoresis

SOD1 aggregates were identified by nondenaturing polyacrylamide gel electrophoresis. Proteins (50 μg) were separated by nondenaturing electrophoresis. Samples were diluted in a 5 × sample buffer without SDS, and the electrophoresis buffer was also without SDS. The samples were then blotted onto a nitrocellulose membrane. The membrane was blocked with 3% bovine serum albumin in T-TBS and incubated for 1 h and 30 min at room temperature with primary anti-SOD1 (1:500; Santa Cruz Biotechnology) and for 1 h at room temperature with secondary antibody horseradish peroxidase-conjugated anti-mouse IgG (1:5000; Sigma–Aldrich). The membrane was developed with the SuperSignal West Pico chemiluminescence substrate (Thermo Scientific), acquired with Chemi-Doc MP (Bio-Rad), and analyzed using Image Lab software (Bio-Rad).

Statistical analysis

Statistical analyses of data obtained by the PD-QUEST software were performed using Student's t test. Significance was accepted if $p < 0.05$. Because the DS/AD PMI was significantly different in comparison to the other three groups we performed linear regression analyses between total protein–HNE modification and PMI to test if total oxidation was affected by the PMI variable. Moreover, to investigate if our experimental data were influenced by genotype

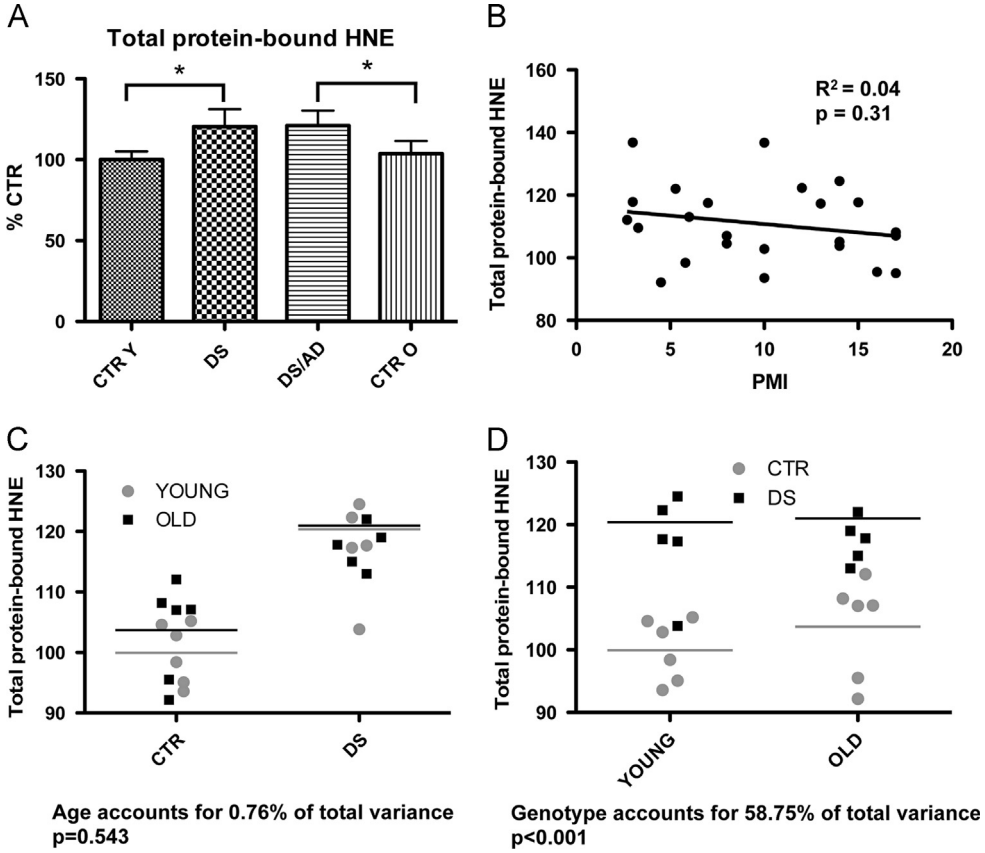

Fig. 1. (A) Total protein-bound HNE levels of CTRY, DS, DS/AD, and CTRO brain samples analyzed by slot-blot assay. Error bars indicate SD for six samples per group. Densitometric values shown are given as percentage with respect to CTRY set as 100% (*$p < 0.05$). (B) Linear regression analysis of total protein-bound HNE levels and PMI. The graph demonstrates no relationship between protein oxidation and PMI ($R^2 = 0.04$; $p = 0.31$). (C and D) Influence of age and genotype, respectively, on protein-bound HNE experimental data.

(DS), age group, or both, and the interaction of such factors, we used a two-way ANOVA (Fig. 1 and Table 3). All statistical analyses were performed using GraphPad Prism 5.0 software.

Results

Protein-bound 4-hydroxy-2-trans-nonenal

The modification of proteins by lipid peroxidation (LPO) -derived products may play a critical role in the pathophysiology of DS. We first determined in our group of samples the variation in the total levels of HNE-bound proteins by slot blot. Considering that DS/AD samples have shorter PMIs, we analyzed whether PMI was a significant contributor to HNE levels and we found that no significant correlation exists between HNE and PMI (Fig. 1B). Our results indicated that oxidative damage, indexed by protein-bound HNE levels, was higher in DS cases overall relative to controls, whereas no significant difference was detected between DS/AD and DS (Fig. 1A). A two-way ANOVA shows that protein-bound HNE levels were influenced by genotype (58.75% of total variance, $p = 0.001$) but not age (0.76% of total variance, $p = 0.543$; Fig. 1C and D).

Based on these findings, we further analyzed our groups by a redox proteomics approach used to identify specific proteins showing increased levels of HNE-modification. Brain homogenates were separated on 2D gels, and HNE-modified proteins were detected by immunoblotting (Figs. 2 and 3). The overall intensities of protein spots that immunoreacted with HNE antibodies appeared higher in both DS/AD and DS compared with their respective controls.

The redox proteomics analyses identified a number of HNE-modified proteins (normalized to expression levels) in the frontal cortex of brain samples when comparing the four groups (Table 2). Further, a two-way ANOVA was used to understand the effects of age and genotype for each protein of interest (Table 3). By comparing the four groups of samples (CTRY, DS, DS/AD, and CTRO) the following results were obtained.

DS vs CTRY

In this group of comparison proteins found to have elevated HNE modification in DS compared to CTRY and identified by MS/MS analysis were cytochrome b–c_1 complex Rieske subunit, mitochondrial (CYT b-c1), with 11.3-fold increase; glial fibrillary acidic protein (GFAP), with 3.7-fold increase; glutamate dehydrogenase 1, mitochondrial (GDH-1), with 1.4-fold increase; peroxiredoxin-2 (Prx2), with 12.3-fold increase; myelin basic protein (MBP), with 11.5-fold increase; ubiquitin carboxyl-terminal hydrolase isozyme L1 (UCH-L1), with 36-fold increase; fructose-bisphosphate aldolase A (FBA-A), with 3.3-fold increase; fructose-bisphosphate aldolase C (FBA-C), with 5.2-fold increase; α-internexin, with 3.2-fold increase; and pyruvate kinase (PK) isozymes M1/M2, with 2.2-fold increase. As expected, the increased oxidation of the majority of the proteins belonging to this group of comparisons is more highly influenced by genotype (presence of DS) than by age group (e.g., GFAP, CYT b-c1; Fig. 2 and Table 3), as the members of our CTRO group were around 60 years of age.

DS/AD vs DS

In this group of comparison proteins showing increased levels of HNE modifications and identified by MS/MS analysis were dihydropyrimidinase-related protein 2 (DRP-2, also called CRMP-2), with 3.4-fold increase; syntaxin-binding protein 1 (SBP1), with 4.8-fold increase; dihydropyrimidinase-related protein 1 (DRP-1, also called CRMP-1), with 4.2-fold increase; GRP78, with 8.3-fold increase; GDH-1, with 3.6-fold increase; MBP, with 5.9-fold increase; aconitate hydratase, mitochondrial, with 11.8-fold increase; and endoplasmin, with 9.5-fold increase. Considering the age difference between DS/AD and DS individuals it is reasonable to expect a contribution of age to the increased oxidative damage observed. Indeed, a two-way ANOVA showed that most of the proteins identified as oxidatively modified in this group of comparisons are significantly influenced by age (Fig. 3 and Table 3).

DS/AD vs CTRO

In this group of proteins differentially HNE-modified, identified by MS/MS analysis, were SOD1, with 3.9-fold increase; CYT b-c1, with 2.9-fold increase; malate dehydrogenase, cytoplasmic (MDH), with 2.4-fold increase; α-enolase, with 7.2-fold increase; septin-11, with 10-fold increase; glyceraldehyde-3-phosphate dehydrogenase (GAPDH), with 15.2-fold increase; DRP-2, with 3.7-fold increase; T-complex protein 1 subunit β, with 13.6-fold increase; SBP1, with 3.8-fold increase; DRP-1, with 9.72-fold increase; heat shock cognate 71-kDa protein (HSC71), with 4.3-fold increase; GRP78, with 35.4-fold increase; neurofilament medium polypeptide (NMP), with 19.1-fold increase; GFAP, with 3.3-fold increase; and GDH-1, with 2.4-fold increase. In the analysis of the influence of age and genotype, we can identify two major subgroups composed of proteins that are oxidatively modified in the DS/AD vs CTRO comparison only or in both DS/AD vs CTRO and DS/AD vs DS comparisons. The proteins identified in the first subgroup, being differentially oxidized in individuals comparable for age, do not show any age-dependency and a two-way ANOVA showed that these are mainly influenced by genotype. In contrast, the proteins identified in the second subgroup show the contribution of both genotype and age to the observed increased HNE modification, as reported by a two-way ANOVA (Fig. 3 and Table 3).

CTRO vs CTRY

The comparison of CTRY vs CTRO was taken into consideration to account for any age effects in the absence of DS. However, only one protein, DRP-2, showed a 2.5-fold increase in aged individuals. Interestingly, DRP-2 was increasingly oxidized across the controls and DS groups and across the comparison of elderly groups (DS/AD and CTRO), thus showing both age and genotype dependence. Indeed, age accounts for 25.2% of the variance ($p = 0.002$) and genotype accounts for 29.7% of the variance ($p = 0.001$; Fig. 2 and Table 3). Table 4 shows a summary of the proteins identified in one or more of the comparison groups.

Immunoprecipitation of GRP78

Data from the validation analysis on GRP78 confirm the increased levels of HNE-bound protein in DS/AD compared to CTRO (2.15- fold), whereas no significant difference was found between DS and CTRY (Fig. 4).

SOD1 levels and aggregates

The analysis of SOD1 expression levels showed an increase in DS (1.5-fold) and DS/AD (1.7-fold) compared to age-matched controls (Fig. 5A). Because SOD1 is encoded on chromosome 21, our data are consistent with previous results from DS brain [27,28] and DS animal models [29].

To test the hypothesis that SOD1 overexpression and oxidative modification may bring about the formation of protein aggregates, we performed native gel electrophoresis. As shown in Fig. 5A and B, SOD1 immunoreactivity under nonreducing conditions corresponds to a band around 90 kDa, thus indicating the formation of protein aggregates. This phenomenon is consistently increased (about 2.3-fold) in DS/AD vs CTRO and correlates with SOD1 oxidation data.

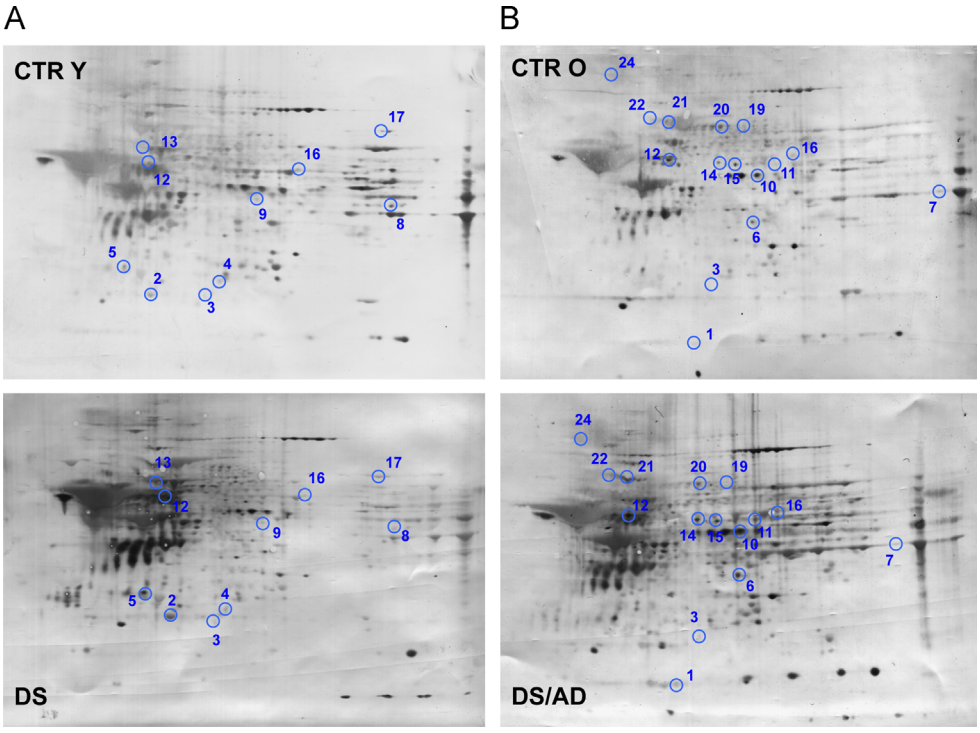

Fig. 2. Proteomic profile of representative 2D blot with proteins differentially oxidized in CTR cases vs DS cases. (A) Comparison between CTRY and DS; (B) comparison between CTRO and DS/AD. The spot numbers are reported in Table 2.

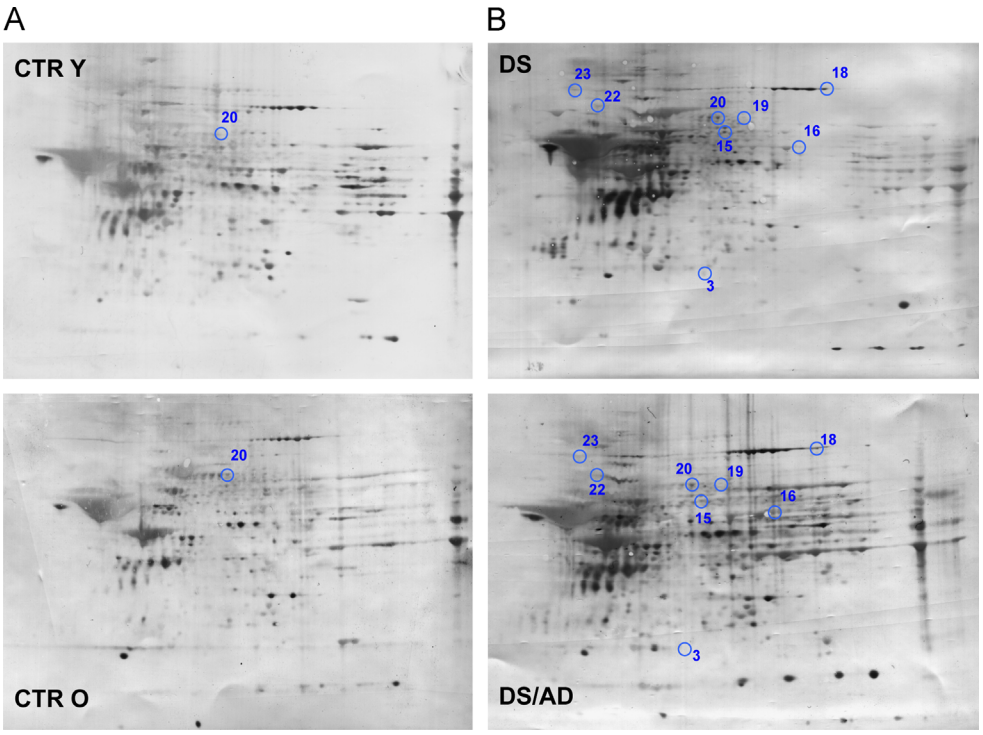

Fig. 3. Proteomic profile of representative 2D blot with proteins differentially oxidized in young cases vs old cases. (A) Comparison between CTRY and CTRO; (B) comparison between DS and DS/AD. The spot numbers are reported in Table 2.

Discussion

The analysis of DS subjects with and without AD pathology [30], compared with their age-matched controls, offers a unique opportunity to discriminate brain dysfunctions associated with oxidative damage, before and after neuropathological manifestation of AD. Results from our group and from others have demonstrated that OS is an early event in the DS phenotype as indexed by increased OS markers in the transgenic animal model of the disease [34], in the amniotic fluid from women carrying DS pregnancy [35], in fetal brain of DS [36], and also from young and adult DS subjects [15,16]. Thus, we analyzed HNE-modified proteins to identify specific

Table 2
HNE-modified proteins in CTRY vs DS, DS vs DS/AD, DS/AD vs CTRO, and CTRO vs CTRY identified by redox proteomics analysis.

Spot	Protein	UniProt No.	% Sequence coverage	Theoretical MW/PI	DS/AD vs CTRO	DS/AD vs DS	DS vs CTRY	CTRO vs CTRY
1	Superoxide dismutase (Cu,Zn)	Q6NR85	77	16,154/5.70	3.9*		*1.2*	
2	Peroxiredoxin-2	P32119	44	22,049/5.66	*2.0*		12.3*	
3	Myelin basic protein	Q6F104	33	33,097/9.79	*1.9*	5.9*	11.5*	
4	Cytochrome b–c_1 complex subunit Rieske, mitochondrial	P47985	21	29,934/8.55	2.9*		11.3*	
5	Ubiquitin carboxyl-terminal hydrolase isozyme L1	P09936	46	25,151/5.33	*1.27*		36*	
7	Malate dehydrogenase, cytoplasmic	36631	25	366,631/6.91	2.4*			
9	Glyceraldehyde-3-phosphate dehydrogenase	P04406	42	36,201/8.57	15.2*		*2.9*	
10	Fructose-bisphosphate aldolase A	P04075	41	39,851/8.30	*2.2*		3.3*	
11	Fructose-bisphosphate aldolase C	P09972	51	39,830/6.41			5.2*	
13	α-Enolase	Q6GMP2	42	47,481/7.01	7.2*		*2.4*	
15	Glial fibrillary acidic protein	Q96KS4	57	49,907/5.42	3.3*		3.7*	
	DnaJ homolog subfamily B member 12	Q9NXW2	23	42,021/8.67				
16	α-Internexin	Q16352	69	55,528/5.34	*1.24*		3.2*	
17	Dihydropyrimidinase-related protein 2	Q16555	31	62,771/5.95	20.3*		*1.3*	2.5*
18	T-complex protein 1 subunit β	P78371	25	57,794/6.01	13.6*		*2.5*	
19	Syntaxin-binding protein 1	P61764	29	67,925/6.49	3.8*	4.8*		
20	Glutamate dehydrogenase 1, mitochondrial	P00367	37	61,701/7.66	2.4*	3.6*	1.4*	
21	Pyruvate kinase isozymes M1/M2	Q96E76	32	58,470/7.96	*1.25*		2.2*	
22	Aconitate hydratase, mitochondrial	Q99798	20	86,113/7.36		11.8*		
25	Dihydropyrimidinase-related protein 1	Q14194	15	62,487/6.55	9.72*	4.2*		
26	Dihydropyrimidinase-related protein 2	Q16555	47	62,771/5.95	3.7*	3.4*	*1.2*	
27	Heat shock cognate 71-kDa protein	P11142	38	71,082/5.37	4.3*		*1.3*	
28	78-kDa glucose-regulated protein	P11021	35	72,402/5.07	35.4*	8.3*	*4.1*	
29	Endoplasmin	P14625	30	92,696/4.76		9.5*		
30	Neurofilament medium polypeptide	P07197	35	102,468/4.90	19.1*		*3.2*	

Italic font indicates a consistent but not significant trend of alteration.

* $p < 0.05$, statistically significant trend.

Table 3
Two-way ANOVA to investigate genotype and age effects on protein-bound HNE experimental data. Bold values are statistically significant; italic bold values are close to significancy.

Target		Two-way ANOVA				
		Age (young–old)		Genotype (DS–DS/AD)		Interaction
No.	Protein	% total var.	p value	% total var.	p value	
1	Superoxide dismutase (Cu,Zn)	2.41	0.42	**16.49**	**0.047**	0.156
2	Peroxiredoxin-2	0.80	0.618	**32.16**	**0.0038**	0.143
3	Myelin basic protein	1.19	0.595	9.38	0.142	0.197
4	Cytochrome b–c_1 complex subunit Rieske, mitochondrial	0.30	0.746	**43.43**	***0.0008**	0.569
5	Ubiquitin carboxyl-terminal hydrolase isozyme L1	2.47	0.421	***15.48***	***0.053***	0.140
6	Malate dehydrogenase, cytoplasmic	6.71	0.216	2.75	0.421	0.207
7	Glyceraldehyde-3-phosphate dehydrogenase	0.27	0.791	**22.96**	**0.023**	0.768
8	Fructose-bisphosphate aldolase A	6.05	0.205	2.76	0.387	**0.025**
9	Fructose-bisphosphate aldolase C	2.71	0.373	10.29	0.091	**0.018**
10	α-Enolase	0.1	0.869	**25.25**	**0.015**	0.356
11	Septin-11	1.57	0.550	3.55	0.372	0.143
12	Glial fibrillary acidic protein	**6.65**	**0.048**	**79.42**	**0.0001**	0.30
13	α-Internexin	0.88	0.654	5.57	0.266	0.181
14	T-complex protein 1 subunit β	2.80	0.435	10.07	0.147	0.706
15	Syntaxin-binding protein 1	**14.44**	**0.038**	***11.09***	***0.066***	**0.033**
16	Glutamate dehydrogenase 1, mitochondrial	**32.90**	**0.0018**	**12.72**	**0.036**	0.244
17	Pyruvate kinase isozymes M1/M2	0.51	0.729	***16.16***	***0.062***	0.839
18	Aconitate hydratase, mitochondrial	**29.35**	**0.0068**	2.97	0.349	0.335
19	Dihydropyrimidinase-related protein 1	3.30	0.35	***12.98***	***0.076***	0.124
20	Dihydropyrimidinase-related protein 2	**25.22**	**0.002**	**29.66**	**0.0001**	**0.001**
21	Heat shock cognate 71-kDa protein	2.16	0.493	6.53	0.239	0.458
22	78-kDa glucose-regulated protein	**13.22**	**0.042**	**24.29**	**0.0082**	0.151
23	Endoplasmin	**29.02**	**0.0037**	**13.03**	**0.039**	0.22
24	Neurofilament medium polypeptide	1.66	0.515	**19.50**	**0.034**	0.374

targets of lipid peroxidation occurring in the frontal cortex as a function of chromosome 21 trisomy, age, and AD pathology. Because protein oxidation alters protein function [37–40], our results suggest molecular mechanisms that are progressively impaired in DS and may drive neurodegenerative phenomena. We compared DS vs CTRY, to characterize the oxidative damage during the pre-AD neuropathology phase in DS phenotype; DS/AD vs DS, to understand oxidized proteins potentially involved in AD progression;

Table 4
Summary table showing proteins identified in one or more groups of comparison.

DS phenotype proteins (DS Y vs CTRY)	AD progression proteins (DS/AD vs DS Y)	Specific AD proteins (DS/AD vs CTRO)
Glutamate dehydrogenase 1, mitochondrial	**Glutamate dehydrogenase 1, mitochondrial**	**Glutamate dehydrogenase 1, mitochondrial**
α-Internexin	**Syntaxin-binding protein 1**	**Syntaxin-binding protein 1**
Ubiquitin carboxyl-terminal hydrolase isozyme L1	**Dihydropyrimidinase-related protein 2**	**Dihydropyrimidinase-related protein 2**
Fructose-bisphosphate aldolase A	**Dihydropyrimidinase-related protein 1**	**Dihydropyrimidinase-related protein 1**
Fructose-bisphosphate aldolase C	**78-kDa glucose-regulated protein**	**78-kDa glucose-regulated protein**
Myelin basic protein	**Myelin basic protein**	Superoxide dismutase 1 (Cu,Zn)
Glial fibrillary acidic protein		
DnaJ homolog subfamily B member 12	Endoplasmin	**Glial fibrillary acidic protein**
DnaJ homolog subfamily B member 12		
Cytochrome *b*–c_1 complex subunit Rieske, mitochondrial	Aconitate hydratase, mitochondrial	**Cytochrome *b*–c_1 complex subunit Rieske, mitochondrial**
Peroxiredoxin-2		T-complex protein 1 subunit β
		Pyruvate kinase isozymes M1/M2
		Heat shock cognate 71-kDa protein
		Neurofilament medium polypeptide
		Glyceraldehyde-3-phosphate dehydrogenase
		α-Enolase
		Malate dehydrogenase, cytoplasmic
		Septin 11

Proteins in boldface appear in more than one group.

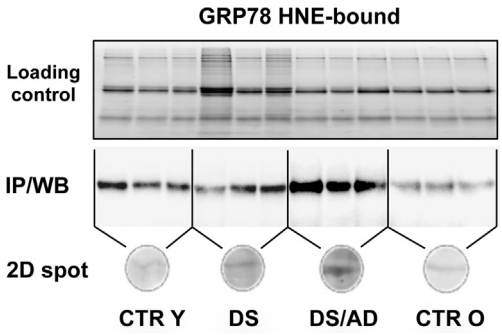

Fig. 4. Protein-bound HNE levels of GRP78 analyzed by immunoprecipitation/Western blot and by 2DE Western blot. Loading control is also shown.

DS/AD vs CTRO, to verify the presence of characteristic oxidative features of AD in DS cases; and finally CTRO vs CTRY, to consider changes that are exclusively age-dependent.

The majority of neurodegenerative disorders are characterized by defects in the cytoskeletal architecture that regulate neuronal shape and trafficking [22]. We identified increased levels of protein-bound HNE of MBP, α-internexin, and GFAP in DS compared to CTRY individuals. This is the first report showing the oxidation of MBP, the major structural protein component of myelin, which plays a functional role in the formation and maintenance of the myelin sheath. Recently, it was demonstrated that MBP binds Aβ and inhibits Aβ fibril formation breakdown in white matter [44–46], which may have relevance to DS. Another member of the cytoskeleton network is α-internexin, a 66-kDa neurofilament protein, involved in the morphogenesis of neurons. Our data may suggest that the increased oxidation of α-internexin, whose expression is already altered in the fetal brain, contributes to the slow and chronic degenerative process of neuronal cells in DS brain. Moreover, α-internexin was found to be HNE bound in studies on the Ts1Cje transgenic mouse for DS [47].

We here demonstrate that UCH-L1, in addition to being increasingly carbonylated [34], is also HNE-modified. UCH-L1 oxidative modification leads to decreased protein functionality [16] and to dysfunction of the protein ubiquitination/deubiquitination machinery, which in turn impairs neuronal function and survival, as already demonstrated in AD brain [16]. Growing evidences indicate that dysfunction of the protein quality control (PQC) system is a key event in triggering neuronal death by favoring the accumulation of oxidized/misfolded proteins. The PQC, through degradation of oxidized/misfolded proteins, provides a critical protective role. If this process is defective, damaged/dysfunctional proteins are not efficiently removed and may accumulate. Indeed, deposits of aggregated, misfolded, and oxidized proteins are key hallmarks of neurodegeneration. Intriguingly, our findings suggest that, in DS brain, the impairment of PQC may be caused by the increased oxidation of selected components of the proteasome, autophagy, and the ubiquitin proteasome system (UPS).

Similarly, GFAP was found to be modified either by increased carbonylation or HNE modification, thus suggesting that this protein is a selective target of oxidative damage. Interestingly, GFAP oxidation was influenced by genotype (Table 3), thus suggesting that its oxidative modifications are associated with trisomy of chromosome 21.

Intellectual disability in DS has often been associated with increased neuronal sensitivity to physiological oxidative radicals and increased susceptibility to undergoing apoptotic death [52]. We found that Prx2 is oxidized in DS brain, which further supports the relationship between a decrease in the antioxidant defense mechanisms and neurodegeneration. Interestingly, previous studies demonstrated that Prx2 was underexpressed in DS fetal brains with respect to controls [53,54]. Furthermore, Hishihara et al. [34] found that another member of this family, Prx6, is HNE-modified in Ts1Cje transgenic mice [55]. In addition, hyperoxidation of Prx2 is found also in DS/AD vs CTRO. Considering that DS brain is under a condition of chronic oxidative stress, resulting from genetic deregulation of chromosome 21, alteration of oxidative defense systems exacerbates the intracellular oxidative burden, thereby favoring the accumulation of oxidized/dysfunctional proteins.

Additional targets of HNE modifications, in DS vs CTRY, are enzymes involved in energy metabolism, including PK M1/M2, FBAs, and CYT b-c1 (complex III subunit 5). Previous findings demonstrate deficient functionality of mitochondrial enzymes [34] and a metabolic deficiency in which an adaptive downregulation of mitochondrial functions occurs [56].

To understand if such deregulation translates into a chronic decrease in the above-mentioned proteins and their associated functions, the comparison of DS/AD and CTRO was undertaken to

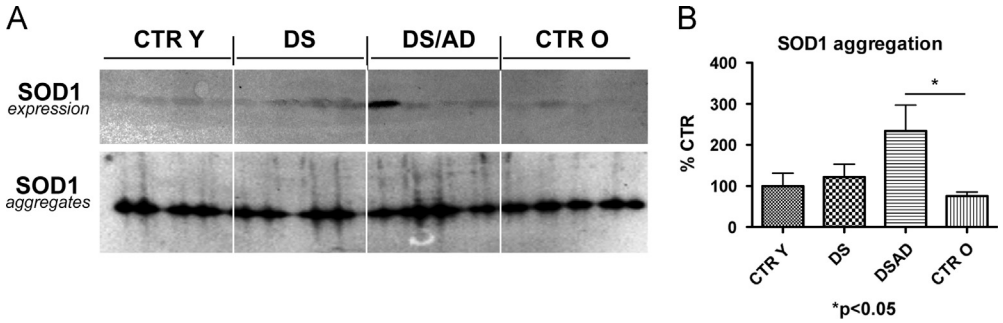

Fig. 5. (A) SOD1 expression levels analyzed by Western blot (top row) and SOD1 aggregates analyzed by native gel electrophoresis (bottom row). (B) Bar graph of SOD1 aggregation in each experimental group. Error bars indicate SD for six samples per group. Densitometric values shown are given as percentage with respect to CTRY set as 100% ($*p < 0.05$).

account for any specific AD differences. Within this context, CYT b-c1 and GFAP were oxidized also in DS/AD, suggesting that the modification of these proteins starts early in the DS population and is still present in DS with AD pathology.

Conversely, SOD1, MDH, GAPDH, septin-11, α-enolase, HSC71, and NMP showed higher levels of oxidation in DS/AD vs CTRO only. Triplication of SOD1 is considered the main factor responsible for increased OS conditions in DS. A recent study by Murakami et al. [60] showed that the SOD1 deficiency in an APP-overexpressing mouse model (Tg2576) accelerates Aβ oligomerization and memory impairment as a consequence of increased oxidative damage. However, the Ts1Cje mice, with a subset of triplicated human chromosome 21 gene orthologs that exclude APP and SOD, show decreases in mitochondrial membrane potential and ATP production, increase in ROS, hyperphosphorylation of tau, increase in GSK3β activity, and unaltered APP metabolism. These findings suggest that genes on the trisomic Ts1Cje segment other than APP and SOD1 can cause oxidative stress, mitochondrial dysfunction, and hyperphosphorylation of tau.

Previous studies from our laboratory [63] demonstrated for the first time that SOD1 is HNE-modified in the inferior parietal lobule of late-stage AD. Protein oxidation often results in the formation of protease-resistant protein aggregates, which are considered highly toxic and can mediate cell death [63]. Considering that SOD1 is overexpressed in DS and also oxidatively modified, we tested the hypothesis that SOD1 aggregates might form and may contribute to neurotoxicity, as well as Aβ fibrils. Moreover, this phenomenon has already been described in an animal model of ALS [64–67], in which mutant SOD1 is overexpressed, oxidatively modified, and aggregated in motor neurons [68]. Intriguingly, our results support the idea that SOD1, similar to what occurs in ALS [69] and also in PD and AD brain [70,71], may bring about the formation of protein aggregates (Fig. 5).

MDH, GAPDH, and α-enolase oxidative modifications are consistent with the chronic dysfunction of energy metabolism that starts early in the young DS population and progresses with aging to DS/AD. Indeed, these proteins have been already identified as oxidatively modified in brain of subjects with AD and mild cognitive impairment [64].

GRP78, DRP-1 and DRP-2, SBP, and GDH-1 were identified as excessively HNE-modified in brain in DS/AD vs CTRO and also DS/AD vs DS, thereby opening an interesting discussion to consider the specific variation caused by aging and those mainly related to genotype. The comparison between the DS/AD and the DS group showed that the majority of the proteins are increasingly oxidized as a function of aging. However, the effect of age is evident only in the DS population, with subtle increases in the CTRO vs the CTRY group (Table 3). These proteins include components of metabolic pathways, antioxidant defense, and axonal guidance that were already discussed elsewhere in the context of AD onset and progression [15]. Further, GRP78, in addition to other mentioned proteins, is a selective target of oxidative damage, because we also identified these proteins to be carbonylated in DS vs CTRY [16]. These data, together with the oxidation of GFAP and UCH-L1, suggest that the impairment of the proteostasis network is an early and characteristic feature of DS neurodegeneration.

If we combine the deregulation of the cytoskeleton network (SBP, NMP, DRP-1, and DRP-2) with energy failure, it is reasonable to hypothesize a stress condition in which mechanisms of neuronal growth, axonal transport, and also neurotransmitter signaling are impaired.

Endoplasmin and aconitate hydratase are increasingly HNE-modified only in the DS/AD group compared with DS alone, and two-way ANOVA supports the notion that age is the major contributor to their oxidative-dependent impairment. Moreover, the effects of normal aging, as indicated by comparing CTRO and CTRY, should be considered as setting the boundary line between normal and pathological aging. Intriguingly, the only protein found to be significantly more oxidized in CTRO than in CTRY is DRP-2, the same protein discussed already to be modulated by an aging effect in the DS/AD vs DS comparison, which overall was influenced by an age effect as reported by two-way ANOVA. However, although our results strongly support the age-dependent susceptibility of DRP-2 to undergoing HNE modification, it is not possible to discriminate between the age- and the genotype-dependent effects.

Conclusions

In conclusion, our study demonstrates that accumulation of oxidatively damaged proteins in the frontal cortex occurs in younger individuals with DS and is higher than in similarly aged non-DS control cases. Accumulation of oxidative damage within neurons is probably responsible for damaging crucial proteins that regulate several processes, including neuronal integrity, axonal transport, synapse connections, degradative systems, energy production, and antioxidant defense. These oxidative stress-related alterations, as demonstrated by us and by a number of other studies, are intrinsically, but not exclusively, dependent on triplication of chromosome 21 genes. We suggest that additional events associated with energy failure and mitochondrial deficits increase as a function of age in DS, driving the neurodegenerative process, which culminates in AD pathology. We speculate that these findings not only are consistent with previous studies in AD, but also may be potential markers of disease progression. However, further molecular studies are needed to further demonstrate the specific role of selected proteins in neurodegeneration.

The comprehension of early events that contribute to and/or regulate the expression of chromosome 21 gene products is a

priority to better understand the mechanisms promoting the development of AD in the DS population, as well as in the general population. Therapeutic strategies based on early pharmacological interventions that modify oxidative stress may be a promising approach to slowing or preventing AD in DS.

Acknowledgments

This work was partially supported by NIH grant to D.A.B. (A6-05119). Brain tissue was acquired by E.H. under funding from the Eunice Kennedy Shriver National Institute of Child Health and Human Development, National Institute on Aging Grant NIH 1RO1HD064993-01. Additional autopsy tissue was obtained from the UCI-ADRC (P50AG16573), from the UK ADC (P30AG28383), and from the NICHD Brain and Tissue Bank for Developmental Disorders of the University of Maryland (Baltimore, MD, USA), Contract HHSN275200900011C (N01HD90011). The content is solely the responsibility of the authors and does not necessarily represent the official views of the National Institutes of Health.

References

[1] Perluigi, M.; Butterfield, D. A. Oxidative stress and Down syndrome: a route toward Alzheimer-like dementia. *Curr. Gerontol. Geriatr. Res.* **2012:**724904; 2012.
[2] Lejeune, J.; Gautier, M.; Turpin, R. [Study of somatic chromosomes from 9 mongoloid children]. *C. R. Hebd. Seances Acad. Sci.* **248:**1721–1722; 1959.
[3] Hassold, T.; Hunt, P. To err (meiotically) is human: the genesis of human aneuploidy. *Nat. Rev. Genet.* **2:**280–291; 2001.
[4] Dierssen, M.; Herault, Y.; Estivill, X. Aneuploidy: from a physiological mechanism of variance to Down syndrome. *Physiol. Rev.* **89:**887–920; 2009.
[5] Wiseman, F. K.; Alford, K. A.; Tybulewicz, V. L.; Fisher, E. M. Down syndrome—recent progress and future prospects. *Hum. Mol. Genet.* **18:**R75–R83; 2009.
[6] Lott, I. T. Neurological phenotypes for Down syndrome across the life span. *Prog. Brain Res.* **197:**101–121; 2012.
[7] Mann, D. M.; Yates, P. O.; Marcyniuk, B.; Ravindra, C. R. The topography of plaques and tangles in Down's syndrome patients of different ages. *Neuropathol. Appl. Neurobiol.* **12:**447–457; 1986.
[8] Wisniewski, K. E.; Dalton, A. J.; McLachlan, C.; Wen, G. Y.; Wisniewski, H. M. Alzheimer's disease in Down's syndrome: clinicopathologic studies. *Neurology* **35:**957–961; 1985.
[9] Leverenz, J. B.; Raskind, M. A. Early amyloid deposition in the medial temporal lobe of young Down syndrome patients: a regional quantitative analysis. *Exp. Neurol.* **150:**296–304; 1998.
[10] Lemere, C. A.; Blusztajn, J. K.; Yamaguchi, H.; Wisniewski, T.; Saido, T. C.; Selkoe, D. J. Sequence of deposition of heterogeneous amyloid β-peptides and APO E in Down syndrome: implications for initial events in amyloid plaque formation. *Neurobiol. Dis.* **3:**16–32; 1996.
[11] Schupf, N.; Sergievsky, G. H. Genetic and host factors for dementia in Down's syndrome. *Br. J. Psychiatry* **180:**405–410; 2002.
[12] Lott, I. T.; Head, E.; Doran, E.; Busciglio, J. Beta-amyloid, oxidative stress and Down syndrome. *Curr. Alzheimer Res.* **3:**521–528; 2006.
[13] Zana, M.; Janka, Z.; Kalman, J. Oxidative stress: a bridge between Down's syndrome and Alzheimer's disease. *Neurobiol. Aging* **28:**648–676; 2007.
[14] Coskun, P. E.; Busciglio, J. Oxidative stress and mitochondrial dysfunction in Down's syndrome: relevance to aging and dementia. *Curr. Gerontol. Geriatr. Res.* **2012:**383170; 2012.
[15] Cenini, G.; Dowling, A. L.; Beckett, T. L.; Barone, E.; Mancuso, C.; Murphy, M. P.; Levine 3rd H.; Lott, I. T.; Schmitt, F. A.; Butterfield, D. A.; Head, E. Association between frontal cortex oxidative damage and beta-amyloid as a function of age in Down syndrome. *Biochim. Biophys. Acta* **1822:**130–138; 2012.
[16] Di Domenico, F.; Coccia, R.; Cocciolo, A.; Murphy, M. P.; Cenini, G.; Head, E.; Butterfield, D. A.; Giorgi, A.; Schinina, M. E.; Mancuso, C.; Cini, C.; Perluigi, M. Impairment of proteostasis network in Down syndrome prior to the development of Alzheimer's disease neuropathology: redox proteomics analysis of human brain. *Biochim. Biophys. Acta* **1832:**1249–1259; 2013.
[17] Butterfield, D. A.; Boyd-Kimball, D. Amyloid beta-peptide(1–42) contributes to the oxidative stress and neurodegeneration found in Alzheimer disease brain. *Brain Pathol.* **14:**426–432; 2004.
[18] Butterfield, D. A.; Drake, J.; Pocernich, C.; Castegna, A. Evidence of oxidative damage in Alzheimer's disease brain: central role for amyloid beta-peptide. *Trends Mol. Med.* **7:**548–554; 2001.
[19] de Haan, J. B.; Cristiano, F.; Iannello, R. C.; Kola, I. Cu/Zn-superoxide dismutase and glutathione peroxidase during aging. *Biochem. Mol. Biol. Int.* **35:**1281–1297; 1995.
[20] Percy, M. E.; Dalton, A. J.; Markovic, V. D.; McLachlan, D. R.; Hummel, J. T.; Rusk, A. C.; Andrews, D. F. Red cell superoxide dismutase, glutathione peroxidase and catalase in Down syndrome patients with and without manifestations of Alzheimer disease. *Am. J. Med. Genet.* **35:**459–467; 1990.
[21] Brugge, K.; Nichols, S.; Saitoh, T.; Trauner, D. Correlations of glutathione peroxidase activity with memory impairment in adults with Down syndrome. *Biol. Psychiatry* **46:**1682–1689; 1999.
[22] Butterfield, D. A.; Stadtman, E. R. Protein oxidation processes in aging brain. *Adv. Cell Aging Gerontol* **2:**161–191; 1997.
[23] Landar, A.; Darley-Usmar, V. M. Nitric oxide and cell signaling: modulation of redox tone and protein modification. *Amino Acids* **25:**313–321; 2003.
[24] Reed, T. T. Lipid peroxidation and neurodegenerative disease. *Free Radic. Biol. Med.* **51:**1302–1319; 2011.
[25] Subramaniam, R.; Roediger, F.; Jordan, B.; Mattson, M. P.; Keller, J. N.; Waeg, G.; Butterfield, D. A. The lipid peroxidation product, 4-hydroxy-2-trans-nonenal, alters the conformation of cortical synaptosomal membrane proteins. *J. Neurochem.* **69:**1161–1169; 1997.
[26] Pedersen, W. A.; Fu, W.; Keller, J. N.; Markesbery, W. R.; Appel, S.; Smith, R. G.; Kasarskis, E.; Mattson, M. P. Protein modification by the lipid peroxidation product 4-hydroxynonenal in the spinal cords of amyotrophic lateral sclerosis patients. *Ann. Neurol.* **44:**819–824; 1998.
[27] Cheon, M. S.; Fountoulakis, M.; Dierssen, M.; Ferreres, J. C.; Lubec, G. Expression profiles of proteins in fetal brain with Down syndrome. *J. Neural Transm. Suppl.* **61:**311–319; 2001.
[28] Gulesserian, T.; Seidl, R.; Hardmeier, R.; Cairns, N.; Lubec, G. Superoxide dismutase SOD1, encoded on chromosome 21, but not SOD2 is overexpressed in brains of patients with Down syndrome. *J. Invest. Med.* **49:**41–46; 2001.
[29] Amano, K.; Sago, H.; Uchikawa, C.; Suzuki, T.; Kotliarova, S. E.; Nukina, N.; Epstein, C. J.; Yamakawa, K. Dosage-dependent over-expression of genes in the trisomic region of Ts1Cje mouse model for Down syndrome. *Hum. Mol. Genet.* **13:**1333–1340; 2004.
[30] Perluigi, M.; Di Domenico, F.; Butterfield, D. A. Unraveling the complexity of neurodegeneration in brain of subjects with Down syndrome: insights from proteomics. *Proteomics Clin. Appl.* **8:**73–85; 2014.
[34] Ishihara, K.; Amano, K.; Takaki, E.; Ebrahim, A. S.; Shimohata, A.; Shibazaki, N.; Inoue, I.; Takaki, M.; Ueda, Y.; Sago, H.; Epstein, C. J.; Yamakawa, K. Increased lipid peroxidation in Down's syndrome mouse models. *J. Neurochem.* **110:**1965–1976; 2009.
[35] Perluigi, M.; di Domenico, F.; Fiorini, A.; Cocciolo, A.; Giorgi, A.; Foppoli, C.; Butterfield, D. A.; Giorlandino, M.; Giorlandino, C.; Schinina, M. E.; Coccia, R. Oxidative stress occurs early in Down syndrome pregnancy: a redox proteomics analysis of amniotic fluid. *Proteomics Clin. Appl.* **5:**167–178; 2011.
[36] Odetti, P.; Angelini, G.; Dapino, D.; Zaccheo, D.; Garibaldi, S.; Dagna-Bricarelli, F.; Piombo, G.; Perry, G.; Smith, M.; Traverso, N.; Tabaton, M. Early glycoxidation damage in brains from Down's syndrome. *Biochem. Biophys. Res. Commun.* **243:**849–851; 1998.
[37] Williams, T. I.; Lynn, B. C.; Markesbery, W. R.; Lovell, M. A. Increased levels of 4-hydroxynonenal and acrolein, neurotoxic markers of lipid peroxidation, in the brain in mild cognitive impairment and early Alzheimer's disease. *Neurobiol. Aging* **27:**1094–1099; 2006.
[38] Reed, T.; Perluigi, M.; Sultana, R.; Pierce, W. M.; Klein, J. B.; Turner, D. M.; Coccia, R.; Markesbery, W. R.; Butterfield, D. A. Redox proteomic identification of 4-hydroxy-2-nonenal-modified brain proteins in amnestic mild cognitive impairment: insight into the role of lipid peroxidation in the progression and pathogenesis of Alzheimer's disease. *Neurobiol. Dis.* **30:**107–120; 2008.
[39] Reed, T. T.; Pierce, W. M.; Markesbery, W. R.; Butterfield, D. A. Proteomic identification of HNE-bound proteins in early Alzheimer disease: insights into the role of lipid peroxidation in the progression of AD. *Brain Res.* **1274:**66–76; 2009.
[40] Butterfield, D. A.; Reed, T.; Perluigi, M.; De Marco, C.; Coccia, R.; Cini, C.; Sultana, R. Elevated protein-bound levels of the lipid peroxidation product, 4-hydroxy-2-nonenal, in brain from persons with mild cognitive impairment. *Neurosci. Lett.* **397:**170–173; 2006.
[44] Epstein, C. J. Epilogue: toward the twenty-first century with Down syndrome—a personal view of how far we have come and of how far we can reasonably expect to go. *Prog. Clin. Biol. Res.* **393:**241–246; 1995.
[45] Holtzman, D. M.; Kilbridge, J.; Chen, K. S.; Rabin, J.; Luche, R.; Carlson, E.; Epstein, C. J.; Mobley, W. C. Preliminary characterization of the central nervous system in partial trisomy 16 mice. *Prog. Clin. Biol. Res.* **393:**227–240; 1995.
[46] Capone, G. T. Down syndrome: advances in molecular biology and the neurosciences. *J. Dev. Behav. Pediatr.* **22:**40–59; 2001.
[47] Sun, Y.; Dierssen, M.; Toran, N.; Pollak, D. D.; Chen, W. Q.; Lubec, G. A gel-based proteomic method reveals several protein pathway abnormalities in fetal Down syndrome brain. *J. Proteomics* **74:**547–557; 2011.
[52] Becker, L.; Mito, T.; Takashima, S.; Onodera, K. Growth and development of the brain in Down syndrome. *Prog. Clin. Biol. Res.* **373:**133–152; 1991.
[53] Helguera, P.; Pelsman, A.; Pigino, G.; Wolvetang, E.; Head, E.; Busciglio, J. ets-2 promotes the activation of a mitochondrial death pathway in Down's syndrome neurons. *J. Neurosci.* **25:**2295–2303; 2005.
[54] Sawa, A. Neuronal cell death in Down's syndrome. *J. Neural Transm. Suppl.* **57:**87–97; 1999.
[55] Sanchez-Font, M. F.; Sebastia, J.; Sanfeliu, C.; Cristofol, R.; Marfany, G.; Gonzalez-Duarte, R. Peroxiredoxin 2 (PRDX2), an antioxidant enzyme, is under-expressed in Down syndrome fetal brains. *Cell. Mol. Life Sci.* **60:**1513–-1523; 2003.
[56] Prince, J.; Jia, S.; Bave, U.; Anneren, G.; Oreland, L. Mitochondrial enzyme deficiencies in Down's syndrome. *J. Neural Transm.: Parkinson's Dis. Dementia Sect.* **8:**171–181; 1994.
[60] Murakami, K.; Murata, N.; Noda, Y.; Tahara, S.; Kaneko, T.; Kinoshita, N.; Hatsuta, H.; Murayama, S.; Barnham, K. J.; Irie, K.; Shirasawa, T.; Shimizu, T. SOD1 (copper/zinc superoxide dismutase) deficiency drives amyloid beta

protein oligomerization and memory loss in mouse model of Alzheimer disease. *J. Biol. Chem.* **286:**44557–44568; 2011.

[63] Perluigi, M.; Sultana, R.; Cenini, G.; Di Domenico, F.; Memo, M.; Pierce, W. M.; Coccia, R.; Butterfield, D. A. Redox proteomics identification of 4-hydroxynonenal-modified brain proteins in Alzheimer's disease: role of lipid peroxidation in Alzheimer's disease pathogenesis. *Proteomics Clin. Appl.* **3:**682–693; 2009.

[64] Nystrom, T. Role of oxidative carbonylation in protein quality control and senescence. *EMBO J.* **24:**1311–1317; 2005.

[65] Chondrogianni, N.; Petropoulos, I.; Grimm, S.; Georgila, K.; Catalgol, B.; Friguet, B.; Grune, T.; Gonos, E. S. Protein damage, repair and proteolysis. *Mol. Aspects Med.* **35:**1–71; 2014.

[66] Grune, T.; Jung, T.; Merker, K.; Davies, K. J. Decreased proteolysis caused by protein aggregates, inclusion bodies, plaques, lipofuscin, ceroid, and 'aggresomes' during oxidative stress, aging, and disease. *Int. J. Biochem. Cell Biol.* **36:**2519–2530; 2004.

[67] Le Pecheur, M.; Bourdon, E.; Paly, E.; Farout, L.; Friguet, B.; London, J. Oxidized SOD1 alters proteasome activities in vitro and in the cortex of SOD1 overexpressing mice. *FEBS Lett.* **579:**3613–3618; 2005.

[68] Furukawa, Y.; Kaneko, K.; Yamanaka, K.; O'Halloran, T. V.; Nukina, N. Complete loss of post-translational modifications triggers fibrillar aggregation of SOD1 in the familial form of amyotrophic lateral sclerosis. *J. Biol. Chem.* **283:**24167––24176; 2008.

[69] Poon, H. F.; Hensley, K.; Thongboonkerd, V.; Merchant, M. L.; Lynn, B. C.; Pierce, W. M.; Klein, J. B.; Calabrese, V.; Butterfield, D. A. Redox proteomics analysis of oxidatively modified proteins in G93A-SOD1 transgenic mice—a model of familial amyotrophic lateral sclerosis. *Free Radic. Biol. Med.* **39:**453––462; 2005.

[70] Bruijn, L. I.; Houseweart, M. K.; Kato, S.; Anderson, K. L.; Anderson, S. D.; Ohama, E.; Reaume, A. G.; Scott, R. W.; Cleveland, D. W. Aggregation and motor neuron toxicity of an ALS-linked SOD1 mutant independent from wild-type SOD1. *Science* **281:**1851–1854; 1998.

[71] Karch, C. M.; Prudencio, M.; Winkler, D. D.; Hart, P. J.; Borchelt, D. R. Role of mutant SOD1 disulfide oxidation and aggregation in the pathogenesis of familial ALS. *Proc. Natl. Acad. Sci. USA* **106:**7774–7779; 2009.